

JPET #122218

Title Page

PDE4B5, a novel, super-short, brain-specific cAMP phosphodiesterase-4 variant whose isoform-specifying N-terminal region is identical to that of cAMP phosphodiesterase-4D6 (PDE4D6)

York-Fong Cheung, Zhengyan Kan, Philip Garrett-Engele, Irene Gall, Hannah Murdoch, George S. Baillie, Luiz Miguel Camargo, Jason M. Johnson, Miles D. Houslay and John C. Castle

Molecular Pharmacology Group, Wolfson Building, Division of Biochemistry and Molecular Biology, Institute of Biomedical & Life Sciences, University of Glasgow, Glasgow, G12 8QQ, Scotland, United Kingdom (YFC, IG, HM, GSB, MDH)

Rosetta Inpharmatics LLC, a wholly owned subsidiary of Merck & Co., Inc., Seattle, Washington, 98109, USA (ZK, PGE, JMJ, JCC)

Merck Research Laboratories, BMB-8-118, 33 Avenue Louis Pasteur, Boston, MA 02115, USA (LMC)

JPET #122218

Running Title Page

Running title: PDE4B5, a novel super-short cAMP phosphodiesterase-4 variant

Corresponding author:

John C. Castle

Rosetta Inpharmatics

401 Terry Ave North, Seattle, Washington 98109

USA

Tel. 1-206-802-6337

Fax 1-206-802-7303

E-Mail: john_castle@merck.com

Section	Cellular and Molecular
Number of text pages	27
Number of tables	3
Number of figures	8
Number of references	59
Number of words in the abstract	219
Number of words in the introduction	655
Number of words in the discussion	940

Non-standard abbreviations:

UCR, upstream conserved regions; DMSO, dimethyl sulfoxide; ORF, open reading frame; DISC1, gene Disrupted In SCHizophrenia 1; PCR, polymerase chain reaction; RT, reverse transcription; DOTAP, Dithiothreitol, *N*--{1-(2,3-Dioleoyloxy)propyl}-*N,N,N*,-trimethylammonium methylsulfate; DTT, dithiothreitol

JPET #122218

Abstract

The cAMP-specific phosphodiesterase-4 (PDE4) gene family is the target of several potential selective therapeutic inhibitors. The four PDE4 genes generate several distinct protein-coding isoforms through the use of alternative promoters and 5' coding exons. Using mouse transcripts, we identified a novel, super-short isoform of human PDE4B encoding a novel 5' terminus, which we label PDE4B5. The protein coding region of the novel 5' exon is conserved across vertebrates, chicken, zebrafish, and fugu. RT-PCR and qPCR measurements show this isoform is brain-specific. The novel protein is 58 ± 2 kDa; has cAMP hydrolyzing enzymatic activity and is inhibited by PDE4 selective inhibitors rolipram and ariflo (cilomilast). Confocal and sub-cellular fractionation analyses show that it is distributed predominantly and unevenly within the cytosol. The 16 novel N-terminal residues of PDE4B5 are identical to the 16 N-terminal residues of the super-short isoform of PDE4D (PDE4D6), which is also brain-specific. PDE4B5 is able to bind the scaffold protein DISC1, whose gene has been linked to schizophrenia. Microarray expression profiling of the PDE4 gene family shows that specific PDE4 genes are enriched in muscle and blood fractions; however, only by monitoring the individual isoforms is the brain-specificity of the super-short PDE4D and PDE4B isoforms revealed. Understanding the distinct tissue specificity of PDE4 isoforms will be important for understanding phosphodiesterase biology and opportunities for therapeutic intervention.

Introduction

Signaling systems coordinate most cellular functions and thus provide key targets for drug discovery. Identifying appropriate targets and generating selective modulators of these targets present major challenges in the initial stages of drug discovery. Different isoenzymes are often found at key control points in signaling networks, allowing cells to tailor signaling pathways through changes in activity, regulation, spatial distribution, and compartmentalization (Wong and Scott, 2004).

The cAMP signaling pathway plays a pivotal role in many key cellular processes (Tasken and Aandahl, 2004; Smith et al., 2006). Indeed, gradients of cAMP have been identified in various cell types (Zhang et al., 2001; Zaccolo and Pozzan, 2002; Willoughby et al., 2006), leading to compartmentalized responses (Tasken and Aandahl, 2004; Wong and Scott, 2004; Smith et al., 2006). Underpinning the formation of such gradients is the degradation of cAMP by phosphodiesterases (PDEs) (Jurevicius et al., 2003; Mongillo et al., 2004; Lynch et al., 2005; McCahill et al., 2005; Willoughby et al., 2006) targeted to specific intracellular sites and signaling complexes (Houslay and Adams, 2003; Baillie and Houslay, 2005). There are many PDE gene families, eight of which code for proteins able to hydrolyze cAMP (Manganiello and Degerman, 1999; Francis et al., 2001; Beavo and Brunton, 2002; Lugnier, 2006). To date, members of the PDE3 and PDE4 families have been shown to play an important role in determining compartmentalized cAMP signaling (Jurevicius et al., 2003; Mongillo et al., 2004; Lynch et al., 2005; McCahill et al., 2005; Willoughby et al., 2006), making it important to appreciate the range of isoforms that form these families as a prelude to determining their functional roles.

The cAMP-specific phosphodiesterase 4 (PDE4) family is the target of several selective inhibitors having therapeutic potential as anti-inflammatory agents, anti-depressants and cognitive enhancers (Huang et al., 2001; O'Donnell and Zhang, 2004; Renau, 2004; Spina, 2004; Houslay et al., 2005). Four genes (PDE4A, PDE4B, PDE4C, PDE4D) generate a large set of PDE4 isoforms through the use of distinct promoters and alternative pre-mRNA splicing (Conti et al., 2003; Houslay and Adams, 2003; Houslay et al., 2005). Their unique N-terminal regions, encoded by specific 5' exons, define individual PDE4 isoforms (Fig. 1). Accordingly, PDE4 isoforms are subcategorized into

JPET #122218

long forms, which possess the regulatory upstream conserved regions, UCR1 and UCR2; short isoforms, which lack UCR1; or super-short isoforms, which lack UCR1 and have a truncated UCR2.

The *PDE4B* gene has been linked to schizophrenia in humans (Millar et al., 2005; Pickard et al., 2007) and knockout of the *PDE4B* gene in mice both generates an anti-depressant-like profile (O'Donnell and Zhang, 2004) and compromises the generation of airway hyper-reactivity and inflammatory actions mediated by macrophages (Jin et al., 2005). Also, chronic nicotine treatment, which has an anti-depressant action, causes down-regulation of PDE4B transcripts in the nucleus accumbens, prefrontal cortex and hippocampus of rats (Polesskaya et al., 2007).

The human *PDE4B* gene has been shown to encode a number of distinct isoforms, namely the long PDE4B1 (Bolger et al., 1993) and PDE4B3 (Huston et al., 1997) isoforms and the short PDE4B2 isoform (Bolger et al., 1993; Obernolte et al., 1993). While an additional long isoform, called PDE4B4, has been identified in rodents, this isoform is not encoded by the human genome (Shepherd et al., 2003). Indeed, particular PDE4 isoforms appear to have specific functional roles as evidenced from siRNA-mediated knockdown studies in cells (Lynch et al., 2005) and from physiological studies showing that nocturnal increases in PDE4B2 provide a negative feedback role in adrenergic/cAMP signalling in the pineal gland (Kim et al., 2007).

Here we identify and characterize the first super-short isoform (PDE4B5) encoded by the *PDE4B* gene. This isoform is highly conserved across species, is active, and responds to drug inhibition. We also show, for the first time, conservation between PDE4 sub-families of an isoform-specific N-terminal region, with the PDE4B5 N-terminal isoform of PDE4B5 being identical to the N-terminus of the super-short isoform encoded by the *PDE4D* gene, PDE4D6 (Wang et al., 2003).

JPET #122218

Methods

Reagents

[³H]-cyclic AMP and ECL were purchased from Amersham International (Amersham, UK). DOTAP and protease inhibitor tablets were obtained from Boehringer Mannheim (Mannheim, Germany). Bradford was purchased from Bio-Rad (Herts, UK). All other materials were from Sigma (Poole, UK). Protein G-sepharose beads was purchased from Amersham Biosciences. Anti-FLAG M2 was supplied by Sigma-Aldrich. PDE4B antisera was as previously described (Huston et al., 1997).

Computational prediction and analysis of PDE4B novel splice variant

Mouse transcripts were aligned to the mouse genome and the orthologous human genomic loci (Kan et al., 2005) and the resulting splice patterns were compared with those of human transcripts to identify novel patterns. Inferred novel splice variant transcript sequences were extracted from the human genome sequence. The nucleotide and translated protein sequences of the variant were searched against NCBI human transcript and protein databases using the on-line BLAST server (<http://www.ncbi.nlm.nih.gov/BLAST/>). Genomic annotations and conservation in the *PDE4B* gene locus were inspected using the UCSC genome browser, hg18 human assembly (<http://genome.ucsc.edu/>). Conserved TFBS predictions were taken from the browser tracks named “HMR Conserved Transcription Factor Binding Sites” by Matt Weirauch and Brian Raney at the University of California at Santa Cruz.

RT-PCR

We used the Qiagen OneStep RT-PCR kit (Qiagen Cat. # 210212). The PCR component involved 35 cycles of 94°C – 30 seconds, 63.5°C – 40 seconds and 72°C – 50 to 120 seconds. Products were resolved on a 2% agarose gel run at 100 volts in TAE buffer. Primer sequences and expected band sizes for PDE4B5, the PDE4B C-terminus, PDE4D6, and the PDE4D N-terminus (excluding PDE4D6) are shown in Table 1. RT-PCR primers were designed to be specific to their target.

TaqMan measurements

JPET #122218

TaqMan primer-probe reagents were obtained through the Applied Biosystems Assays-by-Design custom assay service (Foster City, CA). Probe sequences were designed to straddle the unique splice junction characteristic of each alternative splice form. TaqMan assays were performed on an ABI 7900 real time PCR instrument in 10 μ l assays that were run in triplicate in a 384-well format optical PCR plate. The assays were calibrated with isoform-specific RT-PCR clones using the standard curve method (http://www.appliedbiosystems.com/support/tutorials/pdf/essentials_of_real_time_pcr.pdf). Standard curves generated from plasmid clones were linear across at least six orders of magnitude, and all reported values derived for total tissue RNA fell within the range of these standard curves. RNA was converted to cDNA for TaqMan measurements using a commercially available kit from Applied Biosystems. All assays were normalized on a tissue-to-tissue basis by adding a constant amount of input total RNA into the RT reaction. Taqman primer locations are labeled as 'C' in Fig. 2a.

Microarray data

Custom oligonucleotide microarrays were purchased from Agilent Technologies (Palo Alto, California). We designed these arrays to monitor the expression of 18,000 genes and associated alternate splicing events (Johnson et al., 2003). After alignment of 107,551 full-length human mRNA transcripts to the human genome, probes were designed to target every exon (60mers) and every exon-exon junction (36mers on 10 nucleotide T stilts). Poly[A]⁺ mRNA was amplified with a full-length amplification method using random-priming sequences to reproduce the entire transcript (Castle et al., 2003). Fluorescent dye-labeling, hybridization conditions, and scanning were performed as previously (Hughes et al., 2001). Each amplified sample was hybridized twice against a common reference pool in a dye-swap experiment. The reference pool included 20 disease-free adult tissues, including peripheral leukocytes but excluding other blood fractions. Ratios shown are the mean of three probes located in regions common to all isoforms.

Tissues for RT-PCR, Taqman, and microarray measurements

JPET #122218

Cell lines and human tissues were purchased as mRNA or total RNA from Clontech (Mountain View, California). Each tissue sample was pooled from multiple donors, typically 12, by the vendor.

SDS/PAGE and Western Blotting

Acrylamide gels (4-12%) were used and the samples boiled for 5 min after being resuspended in SDS sample buffer. Gels were run at 100 V/gel for 1-2h with cooling. For detection of transfected PDE by western blotting, 2-50 μ g protein samples were separated by SDS-PAGE and then transferred to nitrocellulose before being immunoblotted using the indicated specific antisera. Labeled bands were identified using peroxidase linked to anti-rabbit IgG and the Amersham ECL western blotting kit was used as a visualization protocol. We used polyclonal antisera able to detect all active human PDE4B isoforms as described previously (Huston et al., 1997). This polyclonal was raised against the extreme C-terminal region that is unique to the PDE4B sub-family and is found in all known active PDE4B isoforms.

Constructs

The ORF encoding human PDE4B5 (EF595686) was engineered for expression in pcDNA3. PDE4B1 (Genbank accession L20966) was used as a PCR template to incorporate the common super-short form region of PDE4B into the new construct. The sequence of the novel 15 N-terminal amino acids of PDE4B5 plus 6 amino acids (249-254) of PDE4B1, a start codon, and a Not1 restriction enzyme site were incorporated into the 5' primer. The 3' primer incorporated amino acids from C-terminal region of PDE4B1, a stop codon and a Kpn1 enzyme restriction site. We also generated a FLAG tagged version where the FLAG tag (N-Asp-Tyr-Lys-Asp-Asp-Asp-Asp-Lys-C) was incorporated into the 3' primer before the stop codon. A PCR reaction using Taq DNA polymerase, PDE4B1 DNA template, and the above primers generated a fragment of approximately 1558 bp, which was purified using PCR Purification Kit (Qiagen, Crawley, UK). This fragment was digested with Not1 and Kpn1 prior to ligation (Rapid DNA ligation Kit, Roche Diagnostic GmbH, Mannheim, Germany) into the multiple

JPET #122218

cloning site (MCS) of pcDNA3.1 (Invitrogen, Paisley, UK) to generate either PDE4B4-pcDNA3 or PDE4B5-FLAG-pcDNA3. Generation of a plasmid encoding N-terminally FLAG epitope-tagged version of the 100kDa full length DISC1 has been described previously (Millar et al., 2005).

Transient expression of PDE4B isoforms in COS7 cells.

Transfection was done using the COS7 SV40-transformed monkey kidney cell line maintained at 37°C in an atmosphere of 5% CO₂ / 95% air in complete growth medium containing DMEM supplemented with 0.1% penicillin/streptomycin (10000 units ml⁻¹), glutamine (2 mM) and 10 % FCS. As described previously (Huston et al., 1997; Rena et al., 2001; Wallace et al., 2005), COS7 cells were transfected using DEAE Dextran. The DNA to be transfected (10 µg) was mixed, and incubated for 15 min with 200 µl of 10 mg ml⁻¹ DEAE-dextran in PBS to give a 'DNA-dextran' mix. When cells reached 70% confluency confluence, in 100 mm dishes, the medium was removed and the cells were given 10 ml of fresh DMEM containing 0.1 mM chloroquine and the DNA-dextran mix (450 µl). The cells were then incubated for 4 h at 37°C. After this period the medium was removed and the cells shocked with 10% DMSO in PBS. After PBS washing, the cells were returned to normal growth medium and left for a further two days before use. For determination of PDE activity the cells were homogenized in KHEM buffer (50 mM KCl, 10 mM EGTA, 1.92 mM MgCl₂, 1 mM dithiothreitol, 50 mM HEPES, final pH7.2,) containing 'complete' protease inhibitors (Boehringer Mannheim) of final concentrations 40 µg ml⁻¹ PMSF, 156 µg ml⁻¹ benzamide hydrochloride, 1 µg ml⁻¹ aprotinin, 1 µg ml⁻¹ leupeptin, 1 µg ml⁻¹ pepstatin A and 1 µg ml⁻¹ antipain. In such transfected cells, >98% of the total PDE activity is due to the recombinant PDE4 isoform (Huston et al., 1997). In some instances the transfected COS7 cells were plated onto 6 well plates for use in experiments and then serum-starved over night before being treated with the indicated ligands for the stated lengths of time.

Sub-cellular fractions.

Disruption of COS7 cells was done as described (McPhee et al., 1995; Bolger et al., 1996; Huston et al., 1997). Cell homogenization was performed in KHEM buffer (50

JPET #122218

mM KCl, 50 mM HEPES, KOH (pH 7.2), 10 mM EGTA, 1.92 mM MgCl₂) containing 1 mM dithiothreitol and a mixture of protease inhibitors at final concentrations of 40 µg/ml PMSF, 156 µg/ml benzamidin, 1 µg/ml aprotinin, 1 µg/ml leupeptin, 1 µg/ml pepstatin A and 1 µg/ml antipain. Pellet fractions were also resuspended in this mixture. We then generated a low-speed, P1 pellet (1000 g_{av} for 10 min) and a high-speed, P2 pellet (60 min at 100000 g_{av}), which left a high-speed supernatant (S2) fraction. The homogenization procedure was complete in that no detectable latent lactate dehydrogenase activity was present in the P1 pellet, indicating an absence of cytosolic proteins. Equal volumes of samples were applied such that detection indicates relative distribution across these three cellular sub-fractions.

Confocal analyses

Confocal imaging for analyzing PDE4 isoforms was performed as described (Rena et al., 2001; Shepherd et al., 2003; Wallace et al., 2005). Here, PDE4B5 was transiently over-expressed and visualized in COS cells using PDE4B specific antisera (Huston et al., 1997). Cells were transfected using DOTAP (Roche, GmbH, Mannheim, Germany), with the PDE4A11- pcDNA3 plasmid. Protein was expressed for 48h and cells were fixed in 4% paraformaldehyde containing 5% sucrose. After permeabilisation in 0.2% triton, proteins were blocked using 10% goat serum and 2% BSA before PDE4A11 was detected using an antibody raised against the C-terminus of human PDE4A and stained using Alexa 594 (Molecular Probes, Invitrogen, Paisley, UK). Cells were observed using a Zeiss Pascal laser scanning microscope.

Immunoprecipitation

HEK293 cells expressing PDE4B5 and/or FlagDISC1 were washed with ice-cold PBS and lysed in PBS containing 1% Triton X-100, 1 mM DTT, 10 mM NaF and 5 mM NaPPi with a protease inhibitor cocktail added (Roche, West Sussex, UK). Lysates were solubilized by rotation on a rotary wheel for 30 min at 4 °C. Insoluble material was removed by a 15 min centrifugation at 14,000 g_{av} at 4 °C followed by pre-clearing of lysed supernatants by incubation with protein G-sepharose beads for 30 min at 4 °C. Equalized amounts of pre-cleared lysates were incubated with the PDE4B antibody for a

JPET #122218

minimum of 3 hours at 4 °C and immunocomplexes were captured following incubation with protein G-sepharose beads for a further 1-2 hours. The immunoprecipitates were washed three times in lysis buffer and eluted from the beads by the addition of Laemmli buffer (Laemmli, 1970).

Assay of cAMP PDE activity

PDE activity using 1 μ M cAMP as substrate was assayed by a modification of the procedure of Thompson and Appleman (1971) and Rutten et al. (1973), as described previously (Marchmont and Houslay, 1980; Sullivan et al., 1998; Rena et al., 2001). All assays were conducted at 30 °C, and, in all experiments, a freshly prepared slurry of Dowex:H₂O:ethanol (1:1:1) was used. In all experiments, initial rates were taken from linear time courses of activity. Dose-dependent inhibition by rolipram was determined in the presence of 1 μ M cAMP concentrations of cAMP as substrate over the indicated range of rolipram concentrations. The IC₅₀ was then determined from these values. Rolipram was dissolved in 100% DMSO as a 1 mM stock and diluted in 20 mM TrisCl, pH 7.4, 10 mM MgCl₂ to provide a range of concentrations in the assay. The residual levels of DMSO were shown not to affect PDE activity over the ranges used in this study.

Protein analysis.

Protein concentration was determined using BSA as standard (Bradford, 1976).

Results

Genomic identification of PDE4B5

Mouse ESTs (e.g., BQ769324) aligned to the human genome indicate a previously unknown 5' exon of the *PDE4B* gene (Methods, Fig. 2a). From the novel first exon splice-site, the 54 nucleotides upstream (in the 5' direction) and the six nucleotides downstream (in the 3' direction) show very high conservation across fifteen species. At the 5' end of this highly conserved sequence exists an in-frame ATG putative start codon (Fig. 2b). The sequence beyond 6 nt upstream of the ATG contains many insertions and deletions across species, as are also present beyond 6 nt downstream of the splice site. However, between the putative start codon and the splice site, no insertions, deletions, or stop codons exist in any of the species examined, including vertebrates, chicken, zebrafish, and fugu. This high rate of protein reading frame evolutionary conservation suggests the existence of a functional protein coding region.

If translated, the alternate first exon would produce a protein of 484 amino acids with a unique N-terminal region of 16 amino acids (Fig. 2c). This protein would preserve the phosphodiesterase catalytic domain but eliminate the 250 N-terminal residues found in long isoforms, replacing them with the novel 16 amino acids. Thus the putative novel PDE4B isoform, which we label PDE4B5, would fall into the category of a super-short isoform (Houslay, 2001), lacking UCR1 and having a truncated UCR2 (Fig. 1).

Intriguingly, BLAST search against the human protein database found that the PDE4B novel variant is homologous to PDE4D6, a recently discovered PDE4D splice variant. The putative protein coding PDE4B5 and PDE4D6 nucleotide sequences show 81% identity (40 of 48 identical nucleotides). Furthermore, the residues of the two unique N-terminus proteins perfectly match over the entire 16 amino acid sequence (Fig. 2c). This, to our knowledge, is the first description of conservation of amino acid sequence over a PDE4 isoform-specific N-terminal region.

Validation and expression of PDE4B5

To validate human transcription of PDE4B5 isoform identified by mouse transcripts, we designed RT-PCR primers targeting the prediction. The forward primer was placed in the unique, novel exon of PDE4B5 and the reverse primer in the PDE4B

JPET #122218

catalytic region (Fig 2a, A; Methods) and both primers were designed to be specific to PDE4B. The gel image shows a bright band at the predicted size (442 nt) in brain sections (fetal brain, cerebellum, frontal lobe, pons, putamen, thalamus and hippocampus) (Fig. 3a). Weaker signals were observed in retina, spinal cord, pituitary, fetal kidney, jejunum, ileum, lung carcinoma A549 cells, testis, HELA cells and G361 melanoma cells, and no band of other size was observed. The RT-PCR gel for total PDE4B expression, using PDE4B-specific probes targeting the shared catalytic unit, shows fairly ubiquitous expression (Fig. 3b). We then quantitatively measured PDE4B5 and PDE4B N-terminus (short and long, but not super-short) transcript levels using TaqMan in four tissues (Fig. 3c.). These measurements show expression of the PDE4B long and short forms in all four tissues while PDE4B5 (super-short) expression is largely constrained to fetal brain, with low levels in cell line A549, in agreement with the RT-PCR gel images.

Subsequent analysis shows only limited homology matches between PDE4B primers and PDE4D. The PDE4B5 forward primer, which lies outside of the coding region, and the PDE4B5 reverse primer, in the PDE4B common catalytic domain, have a maximum continuous homology to the PDE4D locus at a level of four and six nucleotides, respectively. However, even if these matches were to produce products, their size would be significantly different (> 50nt) than the expected 442 nt band.

Given the homology to PDE4D6, we measured PDE4D6 expression using RT-PCR, as per PDE4B5. Again, we designed the forward primer specific to the first exon of PDE4D6, unique to the super-short isoform, and placed the reverse primer in the common catalytic region. We also designed primers to amplify the longer isoforms of PDE4D but not the super-short form, placing the forward primer in the region common to the long and short isoforms but not present in the super-short isoform. The PDE4D6 gel image (Fig.4a) shows expression primarily in brain tissues. The PDE4D long and short gel image (Fig. 4b) shows expression in many tissues, but very low expression in liver, kidney, and K-562.

Given the high expression similarity of PDE4B5 and PDE4D6 isoforms at the sequence and expression level, we examined whether they are similarly regulated. Conservation of the 2000 nucleotides upstream of the common PDE4B5/PDE4D6 ATG

JPET #122218

codon is low but several cross-species conserved transcription factor binding sites are predicted for each isoform. Upstream of PDE4B5, conserved POU1F1, RFX1, RFX, BRN2, and OCT1 binding sites are predicted and upstream of PDE4D6 only SRF is predicted. Thus, these predictions find no common transcription factor binding sites between these two super-short isoforms, suggesting that the expression of these two super-short species is distinctly controlled.

Expression of PDE4 genes in human tissues

We measured the expression of PDE4A, PDE4B, PDE4C, and PDE4D using microarray experiments and show relative expression to a pool of tissues (Fig. 5). The microarray probes were designed to monitor constitutively transcribed exons and junctions, and thus monitor overall gene expression. PDE4A shows slightly higher expression in monocytes, skeletal muscle, testis, and pons. PDE4B shows high enrichment in blood fractions and nervous system tissues. PDE4C shows ubiquitous expression. PDE4D is enriched in blood fractions and skeletal muscle, in agreement with the PDE4D gel image.

Size of PDE4B5 on SDS-PAGE

The ORF of PDE4B5 was engineered for expression in mammalian cells by cloning into pcDNA3. Transfection of COS1 cells with PDE4B5-pcDNA3 allowed for the detection of a single immunoreactive species of 58 ± 2 kDa, detected using a PDE4B specific antiserum (Fig. 6a). Untransfected cells express PDE4B2 at levels not evident at the exposure level used here, which detects only the recombinant species, which is overexpressed so as to provide >98% of total PDE activity in these cells. This size agreed well with a predicted size of 57.7 kDa, as derived from primary amino acid sequence. The short PDE4B2 isoform migrated as a 68 kDa species, as shown previously by us (Huston et al., 1997; Shepherd et al., 2003; Lynch et al., 2005).

Activity of PDE4B5

We transfected cells to express PDE4B5 and treated them with the archetypal PDE4-selective inhibitor, rolipram. Over 97% of the total cAMP PDE activity was

JPET #122218

inhibited by 1 μ M cAMP rolipram as a substrate. Assayed with 1 μ M cAMP, such transfected cells had a cAMP PDE activity of 2-4 nmol cAMP hydrolyzed/min/mg cell protein while empty vector transfected cells had an activity of 4-6 pmol cAMP hydrolyzed/min/mg cell protein (n=3). Thus in PDE4B5-transfected cells, PDE4B5 accounts for > 98% of the total cAMP activity.

Analysis of PDE4B5 activity showed that it had a K_m for cAMP of $5.8 \pm 0.4 \mu$ M (n=3). By analyzing equal immunoreactive amounts of PDE4B5 and PDE4B2, expressed in COS1 cells lysates, we were able to determine the V_{max} of PDE4B5 as $18 \pm 3\%$ of PDE4B2 in these cells.

We then determined the sensitivity of PDE4B5 to inhibition by rolipram and ariflo (cilomilast), a compound that has been in phase 3 clinical trials for COPD (Fig. 7). This gave IC_{50} values of 380 ± 63 nM (n = 4) and 114 ± 17 nM (n = 3), for rolipram and ariflo, respectively. Rolipram binds to the catalytic site of PDE4B, thus providing competitive inhibition. Using the Cheng-Prusoff equation ($K_i = IC_{50}/(1+(S/K_m))$), K_i values for inhibition of PDE4B5 by rolipram and ariflo are 324 and 97 nM, respectively.

Intracellular distribution of PDE4B5

COS1 cells transfected to express PDE4B5 were disrupted and separated out in low speed membrane (P1), high speed membrane (P2) and high speed supernatant (S2) fractions (Fig. 6a). These were then analyzed on a volume for volume basis for both PDE4 activity and for PDE4B5 immunoreactivity to determine the relative distribution of PDE4B5 among these three fractions (Table 2). This analysis showed that PDE4B5 was found predominantly in the high speed supernatant, cytosolic fraction, but was also evidently associated with membrane fractions, which accounted for around 30% of the total PDE4B5 (Table 2).

We also analyzed the distribution of PDE4B5 in transfected COS1 cells (Fig. 6b). As can be seen, while PDE4B5 is excluded from the nucleus, it is distributed throughout the cytosol with small amounts associated with the plasma membrane. Distribution through the cell interior is uneven, which may indicate its association with cytosolic vesicles/complexes in addition to soluble forms. This would be consistent with

JPET #122218

biochemical fractionation. A similar distribution was seen using a FLAG epitope-tagged form of PDE4B5 (Fig. 6b).

PDE4B5 interacts with DISC1.

DISC1 has previously been shown to interact with the long PDE4B1 and PDE4B3 isoforms as well as the short PDE4B2 isoform (Millar et al, 2005). Here we show that the novel, super-short PDE4B5 isoform is able to interact with the full-length 100kDa DISC1 (fl-DISC1) isoform. This is evident from their co-immunoprecipitation as a complex from HEK293 cells that were co-transfected to express both PDE4B5 and fl-DISC1 (Fig. 8).

Discussion

In determining the human transcriptome, the set of human mRNA genes has been largely established and the current need is to establish alternative isoforms, their expression, and their function. To this end, the availability of genomic sequence and RNA transcripts from non-human species is a powerful, complementary resource to human RNA transcripts (Kan et al., 2005).

The human *PDE4B* gene has been shown to encode the long PDE4B1 and PDE4B3 isoforms and the short PDE4B2 isoform (Fig. 1; Table 3). These three isoforms are also seen in rodents, which additionally express the short PDE4B4 isoform, which is not found in humans (Shepherd et al., 2003) (Table 3). Here, we show that mouse EST transcripts predict a novel PDE4B isoform, which we label PDE4B5. This transcript replaces the seven 5' exons of transcript NM_002600 with a single novel 5' exon. Using RT-PCR, we confirmed human transcription of the variant and established that it is expressed specifically in brain sections. The 3' region of this novel exon contains a putative in-frame ATG start codon, followed by a novel 16 residue ORF. That this ORF is conserved in vertebrae, chicken, frog, zebrafish, and fugu strongly suggests a functional role. The protein encoded by this isoform would be 484 residues, would contain the PDE catalytic domain and PDE4B C-terminus, but would lack the UCR1 domain and encode a naked, truncated UCR2 domain. Because the protein would be shorter than the previously identified long and short PDE4B forms, we classify it as a 'super-short' isoform of PDE4B (Houslay, 2001) (Table 3).

By transfecting a PDE4B5 cDNA construct into COS1 cells, we were able to demonstrate that the cDNA generates a protein of 58 ± 2 kDa. Immunoreactivity measurements show that while this protein is found in membranes, it is found dominantly in the cytosol (high speed supernatant fraction). Confocal microscopy immunolocalisation observations of recombinant PDE4B5 using an anti-PDE4B antiserum similarly show a distribution throughout the cytosol with small amounts associated with the plasma membrane. PDE4B5 shows an uneven distribution throughout the cytosol, which may indicate association with cytosolic vesicles/complexes in addition to soluble forms.

JPET #122218

The transfected PDE4B5 cDNA generates an active protein with a K_m for cAMP of $5.8 \pm 0.4 \mu\text{M}$. Rolipram binds in the PDE4 catalytic domain and indeed inhibits activity of this super-short isoform (containing the catalytic domain). Measuring inhibition by rolipram and ariflo, we find IC_{50} values of $380 \pm 63 \text{ nM}$ ($n = 4$) and $114 \pm 17 \text{ nM}$ ($n = 3$), respectively.

Comparing PDE4B5 to other PDE4 genes, we found that the novel 16 residues at the N-terminus of PDE4B5 perfectly match the N-terminus of the recently discovered super-short isoform of PDE4D, called PDE4D6 (Wang et al., 2003). Expanding on previous assessments (Wang et al., 2003), we found that the PDE4D6 transcript, like PDE4B5, is brain specific. However, we identified no common transcription factor binding sites upstream of each isoform, suggesting that these isoforms are independently regulated.

Microarray gene expression profiling shows PDE4B and PDE4D enriched in white blood cell fractions. PDE4D is also over-expressed in skeletal muscle while PDE4B is high in several nervous tissues, including dorsal raphe and hypothalamus, and, to a lesser degree, in muscle. However, what is invisible to these microarray "gene monitoring" experiments is the high specificity of individual isoforms to specific tissues, such as the high specificity of PDE4B5 and PDE4D6 isoforms to brain sections.

Pharmaceutical manipulation of PDE4 genes may aid in treatment of diseases, such as stroke and inflammation, including COPD and asthma. Indeed, PDE4B and PDE4D gene expression is enriched in white-blood cell fractions, possibly suggesting an inflammatory role. PDE4B activity has also been implicated in psychiatric disorders via its interaction with DISC1 (Millar et al., 2005; Pickard et al., 2007), one of the most validated genetic risk factors for schizophrenia (Porteous and Millar, 2006). Indeed, very recently it has been shown that missense mutations in mouse DISC1 that confer depression-like and schizophrenia-like phenotypes interfere with PDE4B binding to DISC1 (Steven et al., 2007). Importantly, knockout of the PDE4B gene in mice yields an anti-depressant-like phenotype (O'Donnell and Zhang, 2004) as does chemical ablation of PDE4 activity using the selective inhibitor rolipram (Wachtel, 1983; Zhang et al., 2002; Zhang et al., 2006; Kanos et al., 2007). Indeed, the anti-depressant phenotype observed upon chronic nicotinic treatment of rats leads to a specific down-regulation of PDE4B transcripts in brain (Polesskaya et al., 2007), consistent with a key role of *PDE4B* in regulating

JPET #122218

depression and psychosis. Both long (PDE4B1, PDE4B3) and short (PDE4B2) short isoforms have been shown to interact with DISC1 and UCR2 identified as a binding site (Millar et al., 2005). Intriguingly, here we show that the super-short PDE4B5 isoform can also interact with DISC1 (Fig. 8). This indicates that either the interaction site in UCR2 lies within the residual portion of the truncated UCR2 found in PDE4B2 or there is an additional site for interaction with DISC1 that lies within the PDE4B catalytic unit. Indeed, recent analyses of various scaffold proteins that serve to sequester PDE4 have identified multiple binding sites (Bolger et al., 2006; Baillie et al., 2007; Sachs et al., 2007; Stefan et al., 2007) and our recent observations (H Murdoch and MD Houslay, unpublished) indicate that the PDE4B catalytic unit does indeed contain a further binding site for fl-DISC1.

Despite the pharmaceutical significance of PDE4, its repertoire of isoforms available to the cell, how these isoforms are regulated, their distinct biological function, and their relationship to disease state are still unclear. Here, we have used mouse transcripts and isoform-specific expression monitoring to discover an intriguing, novel, active, brain-specific PDE4B isoform.

Acknowledgements

JCC thanks Rosetta's Gene Expression Laboratory for microarray data, Sherri Bloomer for project management support, and Chris Raymond and Chris Armour for consultations.

JPET #122218

References

- Baillie GS, Adams DR, Bhari N, Houslay TM, Vadrevu S, Meng D, Li X, Dunlop A, Milligan G, Bolger GB, Klussmann E and Houslay MD (2007) Mapping binding sites for the PDE4D5 cAMP-specific phosphodiesterase to the N- and C-domains of beta-arrestin using spot-immobilized peptide arrays. *Biochem J* **404**:71-80.
- Baillie GS and Houslay MD (2005) Arrestin times for compartmentalised cAMP signalling and phosphodiesterase-4 enzymes. *Curr Opin Cell Biol* **17**:129-134.
- Beavo JA and Brunton LL (2002) Cyclic nucleotide research -- still expanding after half a century. *Nat Rev Mol Cell Biol* **3**:710-718.
- Bolger G, Michaeli T, Martins T, St John T, Steiner B, Rodgers L, Riggs M, Wigler M and Ferguson K (1993) A family of human phosphodiesterases homologous to the dunce learning and memory gene product of *Drosophila melanogaster* are potential targets for antidepressant drugs. *Mol Cell Biol* **13**:6558-6571.
- Bolger GB, Baillie GS, Li X, Lynch MJ, Herzyk P, Mohamed A, Mitchell LH, McCahill A, Hundsrucker C, Klussmann E, Adams DR and Houslay MD (2006) Scanning peptide array analyses identify overlapping binding sites for the signalling scaffold proteins, beta-arrestin and RACK1, in cAMP-specific phosphodiesterase PDE4D5. *Biochem J* **398**:23-36.
- Bolger GB, McPhee I and Houslay MD (1996) Alternative splicing of cAMP-specific phosphodiesterase mRNA transcripts. Characterization of a novel tissue-specific isoform, RNPDE4A8. *J Biol Chem* **271**:1065-1071.
- Bradford MM (1976) A rapid and sensitive method for the quantitation of microgram quantities of protein utilizing the principle of protein-dye binding. *Anal Biochem* **72**:248-254.
- Castle J, Garrett-Engle P, Armour CD, Duenwald SJ, Loerch PM, Meyer MR, Schadt EE, Stoughton R, Parrish ML, Shoemaker DD and Johnson JM (2003) Optimization of oligonucleotide arrays and RNA amplification protocols for analysis of transcript structure and alternative splicing. *Genome Biol* **4**:R66.
- Conti M, Richter W, Mehats C, Livera G, Park JY and Jin C (2003) Cyclic AMP-specific PDE4 Phosphodiesterases as Critical Components of Cyclic AMP Signaling. *J Biol Chem* **278**:5493-5496.

JPET #122218

- Francis SH, Turko IV and Corbin JD (2001) Cyclic nucleotide phosphodiesterases: relating structure and function. *Prog Nucleic Acid Res Mol Biol* **65**:1-52.
- Houslay MD (2001) PDE4 cAMP-specific phosphodiesterases. *Prog Nucleic Acid Res Mol Biol* **69**:249-315.
- Houslay MD and Adams DR (2003) PDE4 cAMP phosphodiesterases: modular enzymes that orchestrate signalling cross-talk, desensitization and compartmentalization. *Biochem J* **370**:1-18.
- Houslay MD, Schafer P and Zhang KY (2005) Keynote review: phosphodiesterase-4 as a therapeutic target. *Drug Discov Today* **10**:1503-1519.
- Huang Z, Ducharme Y, Macdonald D and Robichaud A (2001) The next generation of PDE4 inhibitors. *Curr Opin Chem Biol* **5**:432-438.
- Hughes TR, Mao M, Jones AR, Burchard J, Marton MJ, Shannon KW, Lefkowitz SM, Ziman M, Schelter JM, Meyer MR, Kobayashi S, Davis C, Dai H, He YD, Stephanians SB, Cavet G, Walker WL, West A, Coffey E, Shoemaker DD, Stoughton R, Blanchard AP, Friend SH and Linsley PS (2001) Expression profiling using microarrays fabricated by an ink-jet oligonucleotide synthesizer. *Nat Biotechnol* **19**:342-347.
- Huston E, Lumb S, Russell A, Catterall C, Ross AH, Steele MR, Bolger GB, Perry MJ, Owens RJ and Houslay MD (1997) Molecular cloning and transient expression in COS7 cells of a novel human PDE4B cAMP-specific phosphodiesterase, HSPDE4B3. *Biochem J* **328** (Pt 2):549-558.
- Jin SL, Lan L, Zoudilova M and Conti M (2005) Specific role of phosphodiesterase 4B in lipopolysaccharide-induced signaling in mouse macrophages. *J Immunol* **175**:1523-1531.
- Johnson JM, Castle J, Garrett-Engele P, Kan Z, Loerch PM, Armour CD, Santos R, Schadt EE, Stoughton R and Shoemaker DD (2003) Genome-wide survey of human alternative pre-mRNA splicing with exon junction microarrays. *Science* **302**:2141-2144.
- Jurevicius J, Skeberdis VA and Fischmeister R (2003) Role of cyclic nucleotide phosphodiesterase isoforms in cAMP compartmentation following beta2-

JPET #122218

- adrenergic stimulation of ICa,L in frog ventricular myocytes. *J Physiol* **551**:239-252.
- Kan Z, Garrett-Engle PW, Johnson JM and Castle JC (2005) Evolutionarily conserved and diverged alternative splicing events show different expression and functional profiles. *Nucleic Acids Res* **33**:5659-5666.
- Kanes SJ, Tokarczyk J, Siegel SJ, Bilker W, Abel T and Kelly MP (2007) Rolipram: a specific phosphodiesterase 4 inhibitor with potential antipsychotic activity. *Neuroscience* **144**:239-246.
- Kim JS, Bailey MJ, Ho AK, Moller M, Gaildrat P and Klein DC (2007) Daily rhythm in pineal phosphodiesterase (PDE) activity reflects adrenergic/3',5'-cyclic adenosine 5'-monophosphate induction of the PDE4B2 variant. *Endocrinology* **148**:1475-1485.
- Laemmli UK (1970) Cleavage of structural proteins during the assembly of the head of bacteriophage T4. *Nature* **227**:680-685.
- Lugnier C (2006) Cyclic nucleotide phosphodiesterase (PDE) superfamily: a new target for the development of specific therapeutic agents. *Pharmacol Ther* **109**:366-398.
- Lynch MJ, Baillie GS, Mohamed A, Li X, Maisonneuve C, Klussmann E, van Heeke G and Houslay MD (2005) RNA silencing identifies PDE4D5 as the functionally relevant cAMP phosphodiesterase interacting with beta arrestin to control the protein kinase A/AKAP79-mediated switching of the beta2-adrenergic receptor to activation of ERK in HEK293B2 cells. *J Biol Chem* **280**:33178-33189.
- Manganiello VC and Degerman E (1999) Cyclic nucleotide phosphodiesterases (PDEs): diverse regulators of cyclic nucleotide signals and inviting molecular targets for novel therapeutic agents. *Thromb Haemost* **82**:407-411.
- Marchmont RJ and Houslay MD (1980) A peripheral and an intrinsic enzyme constitute the cyclic AMP phosphodiesterase activity of rat liver plasma membranes. *Biochem J* **187**:381-392.
- McCahill A, McSorley T, Huston E, Hill EV, Lynch MJ, Gall I, Keryer G, Lygren B, Tasken K, van Heeke G and Houslay MD (2005) In resting COS1 cells a dominant negative approach shows that specific, anchored PDE4 cAMP phosphodiesterase isoforms gate the activation, by basal cyclic AMP production,

JPET #122218

- of AKAP-tethered protein kinase A type II located in the centrosomal region. *Cell Signal* **17**:1158-1173.
- McPhee I, Pooley L, Lobban M, Bolger G and Houslay MD (1995) Identification, characterization and regional distribution in brain of RPDE-6 (RNPDE4A5), a novel splice variant of the PDE4A cyclic AMP phosphodiesterase family. *Biochem J* **310** (Pt 3):965-974.
- Millar JK, Pickard BS, Mackie S, James R, Christie S, Buchanan SR, Malloy MP, Chubb JE, Huston E, Baillie GS, Thomson PA, Hill EV, Brandon NJ, Rain JC, Camargo LM, Whiting PJ, Houslay MD, Blackwood DH, Muir WJ and Porteous DJ (2005) DISC1 and PDE4B are interacting genetic factors in schizophrenia that regulate cAMP signaling. *Science* **310**:1187-1191.
- Mongillo M, McSorley T, Evellin S, Sood A, Lissandron V, Terrin A, Huston E, Hannawacker A, Lohse MJ, Pozzan T, Houslay MD and Zaccolo M (2004) Fluorescence resonance energy transfer-based analysis of cAMP dynamics in live neonatal rat cardiac myocytes reveals distinct functions of compartmentalized phosphodiesterases. *Circ Res* **95**:67-75.
- O'Donnell JM and Zhang HT (2004) Antidepressant effects of inhibitors of cAMP phosphodiesterase (PDE4). *Trends Pharmacol Sci* **25**:158-163.
- Oberholte R, Bhakta S, Alvarez R, Bach C, Zuppan P, Mulkins M, Jarnagin K and Shelton ER (1993) The cDNA of a human lymphocyte cyclic-AMP phosphodiesterase (PDE IV) reveals a multigene family. *Gene* **129**:239-247.
- Pickard BS, Thomson PA, Christoforou A, Evans KL, Morris SW, Porteous DJ, Blackwood DH and Muir WJ (2007) The PDE4B gene confers sex-specific protection against schizophrenia. *Psychiatr Genet* **17**:129-133.
- Polesskaya OO, Smith RF and Fryxell KJ (2007) Chronic nicotine doses down-regulate PDE4 isoforms that are targets of antidepressants in adolescent female rats. *Biol Psychiatry* **61**:56-64.
- Porteous DJ and Millar JK (2006) Disrupted in schizophrenia 1: building brains and memories. *Trends Mol Med* **12**:255-261.

JPET #122218

- Rena G, Begg F, Ross A, MacKenzie C, McPhee I, Campbell L, Huston E, Sullivan M and Houslay MD (2001) Molecular cloning and characterization of the novel cAMP specific phosphodiesterase, PDE4A10. *Mol. Pharmacol.* **59**:996-1011.
- Renau TE (2004) The potential of phosphodiesterase 4 inhibitors for the treatment of depression: opportunities and challenges. *Curr Opin Investig Drugs* **5**:34-39.
- Rutten WJ, Schoot BM and De Pont JJHM (1973) Adenosine 3',5'-monophosphate phosphodiesterase assay in tissue homogenates. *Biochim. Biophys. Acta* **315**:378-383.
- Sachs BD, Baillie GS, McCall JR, Passino MA, Schachtrup C, Wallace DA, Dunlop A, J., MacKenzie KF, Klussmann E, Lynch MJ, Sikorski SL, Nuriel T, Tsigelny I, Zhang J, Houslay MD, Chao MV and Akassoglou K (2007) p75 Neurotrophin receptor regulates tissue fibrosis through inhibition of plasminogen activation via a PDE4/cAMP/PKA pathway. *J. Cell Biol.* **in press**.
- Shepherd M, McSorley T, Olsen AE, Johnston LA, Thomson NC, Baillie GS, Houslay MD and Bolger GB (2003) Molecular cloning and subcellular distribution of the novel PDE4B4 cAMP-specific phosphodiesterase isoform. *Biochem J* **370**:429-438.
- Siepel A, Bejerano G, Pedersen JS, Hinrichs AS, Hou M, Rosenbloom K, Clawson H, Spieth J, Hillier LW, Richards S, Weinstock GM, Wilson RK, Gibbs RA, Kent WJ, Miller W and Haussler D (2005) Evolutionarily conserved elements in vertebrate, insect, worm, and yeast genomes. *Genome Res* **15**:1034-1050.
- Smith FD, Langeberg LK and Scott JD (2006) The where's and when's of kinase anchoring. *Trends Biochem Sci* **31**:316-323.
- Spina D (2004) The potential of PDE4 inhibitors in respiratory disease. *Curr Drug Targets Inflamm Allergy* **3**:231-236.
- Stefan E, Wiesner B, Baillie GS, Mollajew R, Henn V, Lorenz D, Furkert J, Santamaria K, Nedvetsky P, Hundsrucker C, Beyermann M, Krause E, Pohl P, Gall I, MacIntyre AN, Bachmann S, Houslay MD, Rosenthal W and Klussmann E (2007) Compartmentalization of cAMP-dependent signaling by phosphodiesterase-4D is involved in the regulation of vasopressin-mediated water reabsorption in renal principal cells. *J Am Soc Nephrol* **18**:199-212.

JPET #122218

- Steven J, Clapcote SJ, Lipina TV, Millar JK, Mackie S, Christie S, Ogawa F, Lerch JP, Trimble K, Uchiyama M, Sakuraba Y, Kaneda H, Shiroishi T, Houslay MD, Henkelman RM, Sled JG, Gondo Y, Porteous DJ and Roder JC (2007) Behavioural phenotypes of *Disc1* missense mutations in mice. *Neuron* **in press**.
- Sullivan M, Rena G, Begg F, Gordon L, Olsen AS and Houslay MD (1998) Identification and characterization of the human homologue of the short PDE4A cAMP-specific phosphodiesterase RD1 (PDE4A1) by analysis of the human HSPDE4A gene locus located at chromosome 19p13.2. *Biochem J* **333**:693-703.
- Tasken K and Aandahl EM (2004) Localized effects of cAMP mediated by distinct routes of protein kinase A. *Physiol Rev* **84**:137-167.
- Thompson WJ and Appleman MM (1971) Multiple cyclic nucleotide phosphodiesterase activities from rat brain. *Biochemistry* **10**:311-316.
- Wachtel H (1983) Potential antidepressant activity of rolipram and other selective cyclic adenosine 3',5'-monophosphate phosphodiesterase inhibitors. *Neuropharmacology* **22**:267-272.
- Wallace DA, Johnston LA, Huston E, MacMaster D, Houslay TM, Cheung YF, Campbell L, Millen JE, Smith RA, Gall I, Knowles RG, Sullivan M and Houslay MD (2005) Identification and characterization of PDE4A11, a novel, widely expressed long isoform encoded by the human PDE4A cAMP phosphodiesterase gene. *Mol Pharmacol* **67**:1920-1934.
- Wang D, Deng C, Bugaj-Gaweda B, Kwan M, Gunwaldsen C, Leonard C, Xin X, Hu Y, Unterbeck A and De Vivo M (2003) Cloning and characterization of novel PDE4D isoforms PDE4D6 and PDE4D7. *Cell Signal* **15**:883-891.
- Willoughby D, Wong W, Schaack J, Scott JD and Cooper DM (2006) An anchored PKA and PDE4 complex regulates subplasmalemmal cAMP dynamics. *Embo J* **25**:2051-2061.
- Wong W and Scott JD (2004) AKAP signalling complexes: focal points in space and time. *Nat Rev Mol Cell Biol* **5**:959-970.
- Zaccolo M and Pozzan T (2002) Discrete microdomains with high concentration of cAMP in stimulated rat neonatal cardiac myocytes. *Science* **295**:1711-1715.

JPET #122218

- Zhang HT, Huang Y, Jin SL, Frith SA, Suvarna N, Conti M and O'Donnell JM (2002) Antidepressant-like profile and reduced sensitivity to rolipram in mice deficient in the PDE4D phosphodiesterase enzyme. *Neuropsychopharmacology* **27**:587-595.
- Zhang HT, Zhao Y, Huang Y, Deng C, Hopper AT, De Vivo M, Rose GM and O'Donnell JM (2006) Antidepressant-like effects of PDE4 inhibitors mediated by the high-affinity rolipram binding state (HARBS) of the phosphodiesterase-4 enzyme (PDE4) in rats. *Psychopharmacology (Berl)* **186**:209-217.
- Zhang J, Ma Y, Taylor SS and Tsien RY (2001) Genetically encoded reporters of protein kinase A activity reveal impact of substrate tethering. *Proc Natl Acad Sci U S A* **98**:14997-15002.

JPET #122218

Footnotes

MDH thanks the Medical Research Council (UK) (G8604010) for financial support.

ZK is currently at Genentech, Inc., 1 DNA Way, South San Francisco, CA 94080, USA.

JPET #122218

Legends for Figures

Figure 1. PDE4B isoforms.

PDE4 isoforms encoded by the human PDE4B gene. Indicated are the N-terminal regions unique to each isoform, the regulatory Upstream Conserved Regions, UCR1 and UCR2, the Linker Regions, LR1 and LR2, together with the catalytic unit and the PDE4B-specific C-terminal region. Isoforms are grouped as long forms that have both UCR1 and UCR2, short forms that lack UCR1, and super-short forms that both lack UCR1 and have a truncated UCR2. Isoforms are PDE4B1 (human, M25350; rat, AF202732), PDE4B2 (human, M28413; rat, L27058), PDE4B3 (human, L27058; rat, U95748) and PDE4B5 (human submission pending). PDE4B4 (rat, AF202732) isoform is found in rodents and not shown here.

Figure 2. Bioinformatics identification of PDE4B5.

(a) Human genomic alignment of the human transcript NM_002600 and mouse EST BQ769324, including the novel 5' exon (red). A and B show RT-PCR primer locations and C shows Taqman probe sites. (b) Genomic sequence underlying the novel first exon, showing high conservation in 15 species in the putative protein coding region (Siepel et al., 2005). (c) Protein translation of the novel PDE4B5 variant, with novel sequence shown in red italics, aligned to PDE4D6 (super-short isoform).

Figure 3. PDE4B5 expression

(a) Expression of PDE4B5 using RT-PCR. (b) Expression of the PDE4B catalytic unit, found in all PDE4B isoforms. (c) Taqman measurements of the PDE4B5 and the PDE4B long-isoform N-terminus. The expression level is normalized to the highest observed expression. Primer locations for all experiments are indicated in Figure 2a.

Figure 4. PDE4D6 expression

(a) Expression of PDE4D6 using RT-PCR. Tissues are arranged as per Figure 3a. (b) Expression of the PDE4D catalytic unit, found in all PDE4D isoforms.

JPET #122218

Figure 5. Microarray expression of PDE4 genes

Figure 6. Immunodetection of recombinant PDE4B5 expressed in mammalian cells.

(a) Immunoblot detection of recombinant PDE4B2 and PDE4B5 in lysates from transfected COS1 cells identifying PDE4B immunoreactivity in the P1, P2 and S2 fractions with analysis of mock transfected cells also shown. Loading of P1, P2 and S2 fractions were done on an equal volume basis with identical amounts of protein loading for the untransfected and transfected cells in the S2 fraction and with equal exposure to allow comparison. (b) Immunolocalisation by confocal microscopy of recombinant PDE4B5 expressed in COS1 cells as either untagged form, detected with anti-PDE4B antiserum, or FLA epitope-tagged from, with anti-FLAG antibody.

Figure 7. Inhibition of PDE4B5 by rolipram and ariflo

Dose response curves for inhibition of recombinant PDE4B5 activity expressed in COS1 cells lysates and assayed with 1 μ M cAMP substrate for (a) rolipram and (b) ariflo. The examples shown are typical of plots done on 3 separate occasions.

Figure 8. Co-immunoprecipitation of the full-length DISC1 with PDE4B5

PDE4B5 and N-terminally FLAG-tagged full length 100kDa DISC1 were expressed in various combinations in HEK293 cells. Anti-PDE4B immunoprecipitates were resolved by SDS-PAGE and immunoblotted to detect the FLAG tag (upper panel). Similar levels of immuno-capture of PDE4B5 were determined by immunoblotting with the PDE4B antibody (lower panel). The relative expression levels of Flag-tagged full-length DISC1 and PDE4B5 in ~5% of total cell lysate input used for co-immunoprecipitation assays were determined by direct immunoblotting with the PDE4B antisera (lower panel) and the anti-FLAG M2 antibody (upper panel). IP – immunoprecipitate; IB – immunoblot.

JPET #122218

Tables

Table 1. RT-PCR primers

	Size	Forward primer	Reverse primer
PDE4B5 only	442	ACTGTGAATTCCTTCAAAGGGATTGTG	GGTCTATTGTGAGAATATCCAGCCACAT
PDE4B catalytic	431	TGTCTTCACAGATTTGGAGATCCTGGCT	CGGTCTGTCCATTGCCGATACAATTC
PDE4D6 only	276	AAACTATTTACTGTCAGTGTCTTGGGGCTAC	TTAACTCCAAACCTTGGGATACTTGAATTAGT
PDE4D not super-short	242	CTAGAGACCCTACAGACCAGGCACTC	ATCAATTCTTGACTCCACTGATCTGAGACAT

JPET #122218

Table 2. Intracellular distribution of recombinant PDE4B5.

COS1 cells were transfected to express PDE4B5, and its distribution between low speed pellet (P1), high speed pellet (P2), and high speed supernatant (S2) cytosolic fractions was assessed. This distribution was followed by determining PDE4 activity both by using 1 μ M cAMP as substrate and immunologically by using a PDE4B specific antiserum to follow the distribution of the 58 kDa PDE4B5. Data show means and standard deviations for 3 separate experiments.

<i>Fraction</i>	<i>activity distribution (%)</i>	<i>blot distribution (%)</i>
P1	13 \pm 2	12 \pm 2
P2	17 \pm 2	15 \pm 2
S2	70 \pm 7	73 \pm 7

JPET #122218

Table 3. PDE4B isoforms

Lists the currently know range of PDE4B isoforms together with their apparent size from migration on SDS-PAGE, their category and Genbank Accession numbers. Given are data for human isoforms, except for PDE4B4, which is not encoded by the human genome but is found in rodent genomes, with data given here for rat PDE4B4*. The category of PDE4 isoforms are as defined in Houslay, 2001.

Isoform	Size on SDS-PAGE (kDa)	Category	Genbank
PDE4B1	104	Long	L20966
PDE4B2	68	Short	M97515, L20971
PDE4B3	103	Long	U85048
PDE4B4*	84	Long	AF202733
PDE4B5	58	Super-short	EF595686

Figure 1

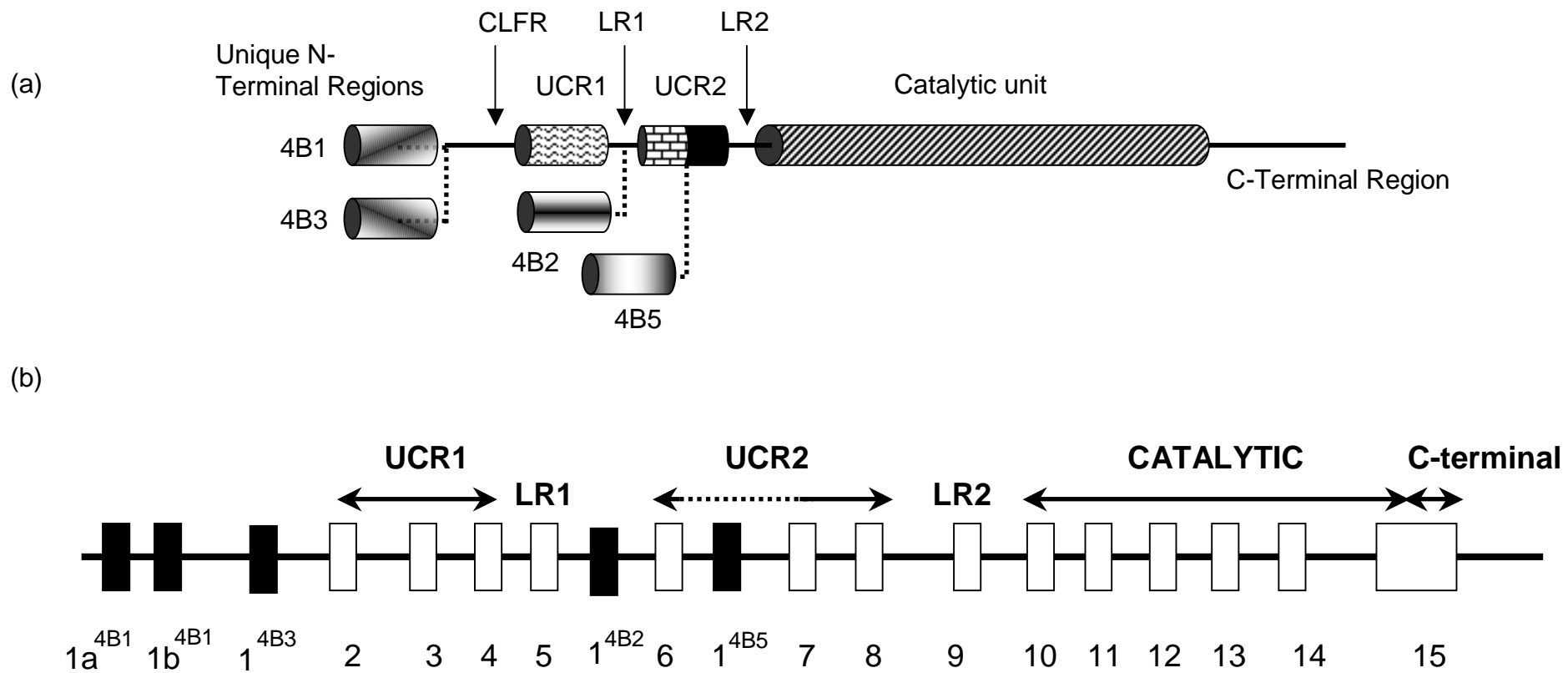
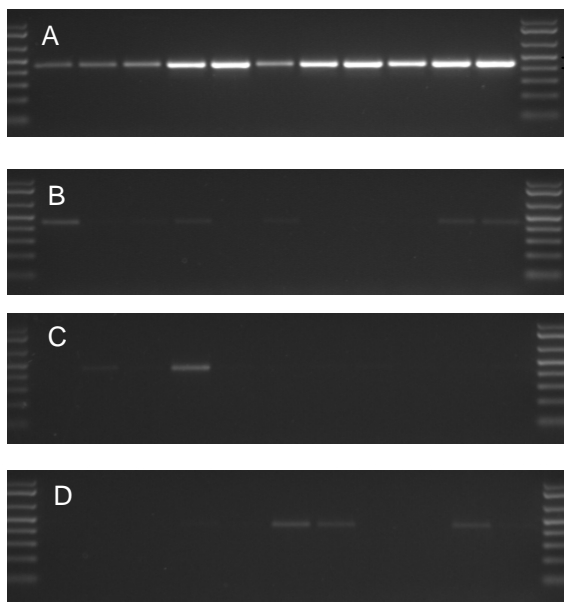


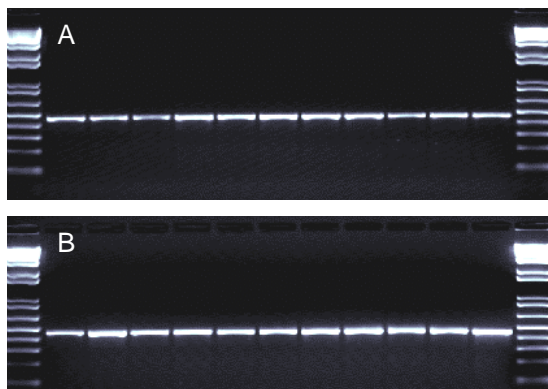
Figure 3

A. PDE4B5 (N-terminus)



Retina	A 1	Fetal Kidney	B 1
Pituitary	2	Fetal Liver	2
Spinal Cord	3	Fetal Lung	3
Brain, Cerebellum	4	Fetal Vertebra	4
Brain, Frontal Lobe	5	Heart	5
Brain, Medulla Oblongata	6	Kidney	6
Brain, Pons	7	Liver	7
Brain, Putamen	8	Pancreas	8
Brain, Thalamus	9	Stomach	9
Brain, Hippocampus	10	Jejunum	10
Fetal Brain	11	Ileum	11
Colon, descending	C 1	Bone Marrow	D 1
Colon tumor tissue	2	Peripheral Leukocytes	2
Lung	3	Uterus	3
Lung Carcinoma (A549)	4	Placenta	4
Prostate	5	Ovary	5
Thyroid	6	Testis	6
Adipose	7	Hela S3	7
Skin	8	Leukemia (K-562)	8
Skeletal Muscle	9	Lymphoma Burkitt's (Raji)	9
Adrenal Gland	10	Melanoma (G361)	10
Thymus	11	Osteosarcoma (MG-63)	11

B. PDE4B C-terminus



Heart	A 1	Lymphoma (Raji)	B 1
Kidney	2	Spinal cord	2
Liver	3	Lymph node	3
Brain	4	Kidney - fetal	4
Placenta	5	Uterus	5
Lung	6	Spleen	6
Brain - fetal	7	Brain - thalamus	7
Leukemia (HL-60)	8	Lung - fetal	8
Adrenal medulla	9	Testis	9
Liver - fetal	10	Melanoma (G361)	10
Salivary gland	11	Lung carcinoma (A549)	11

C. Taqman

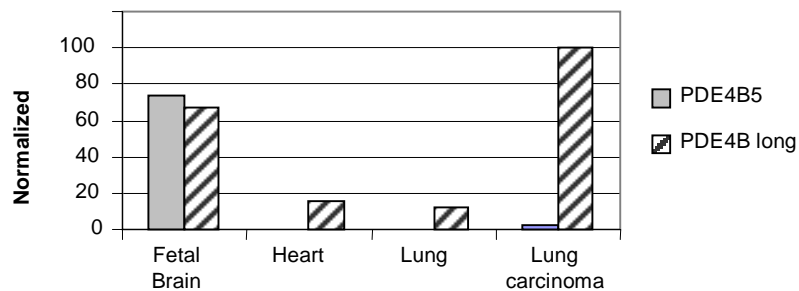


Figure 4

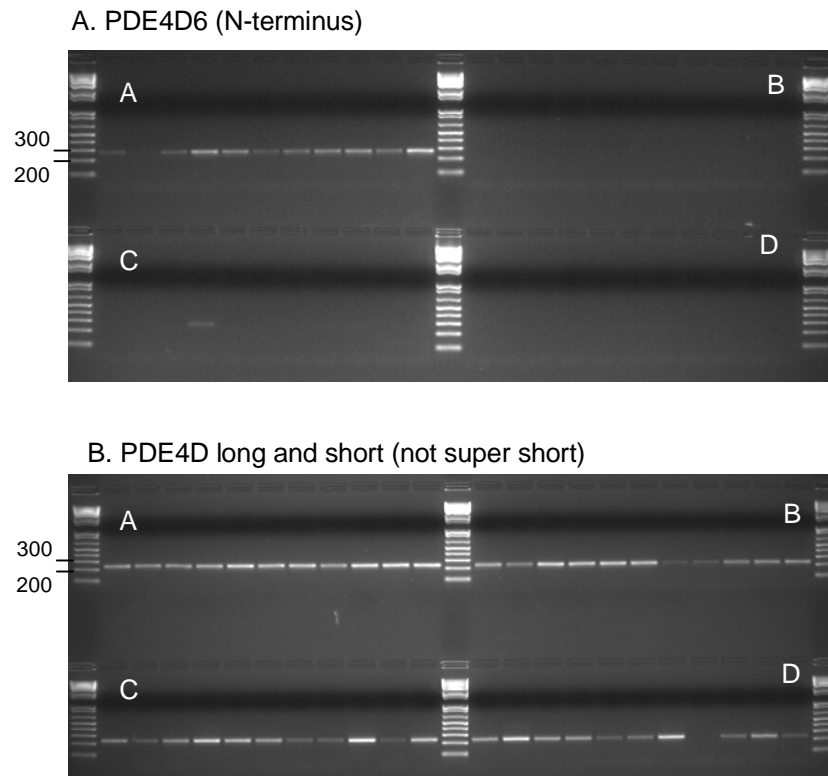


Figure 5

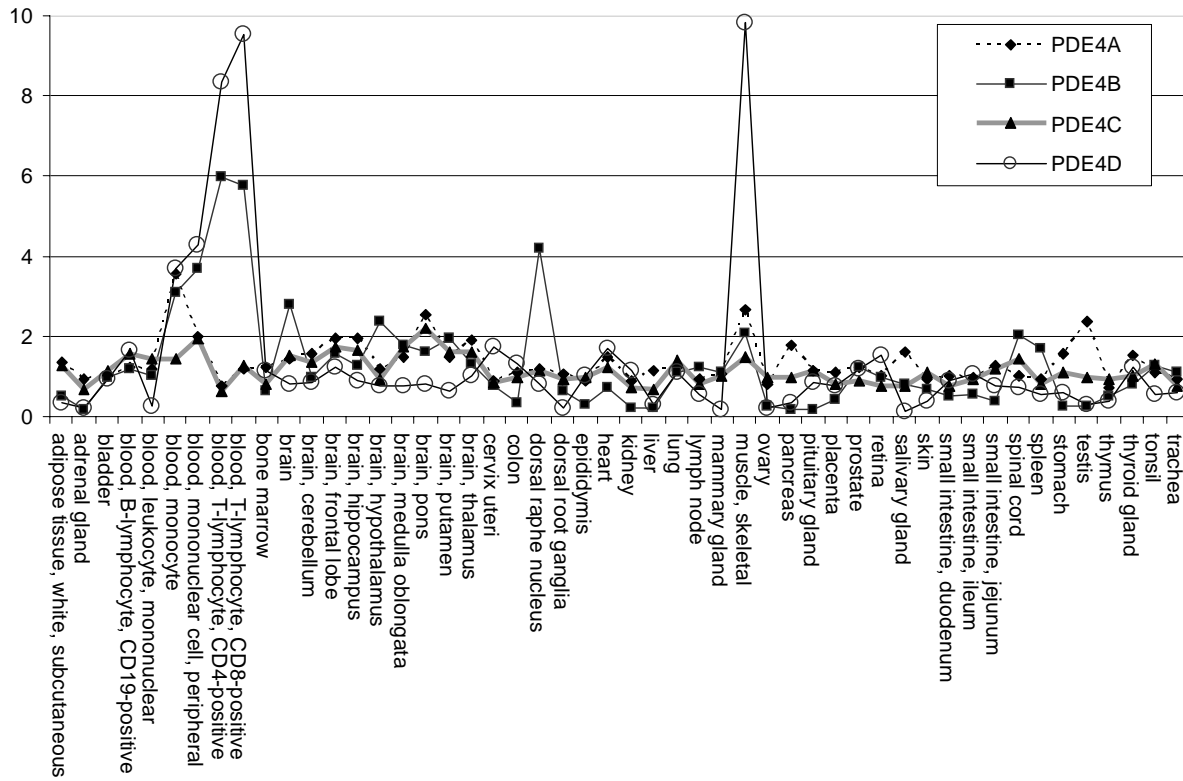
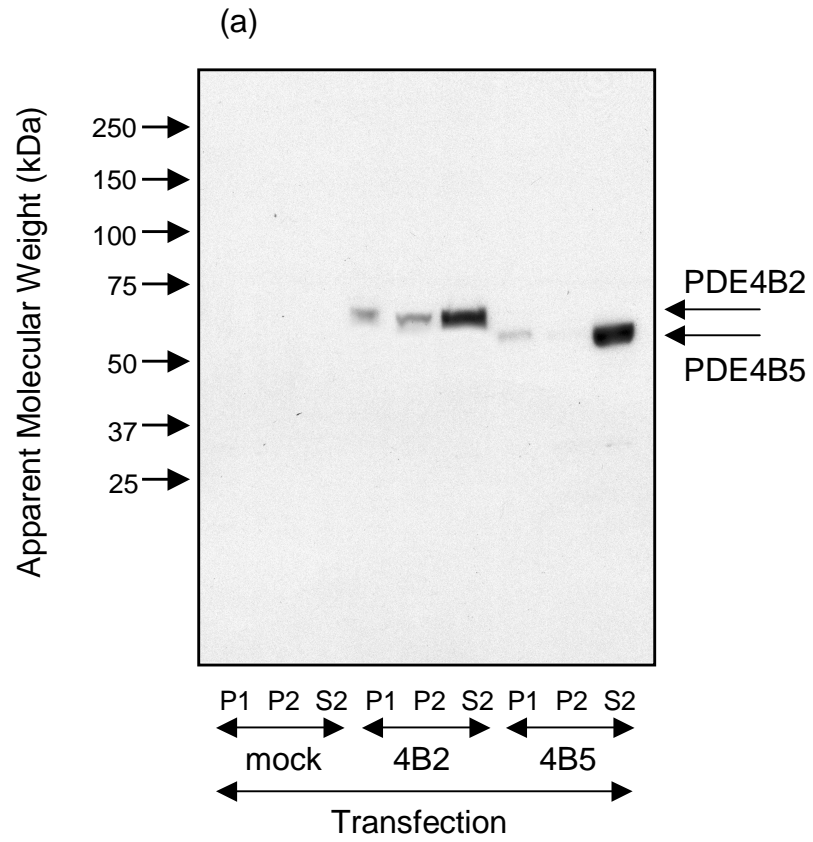
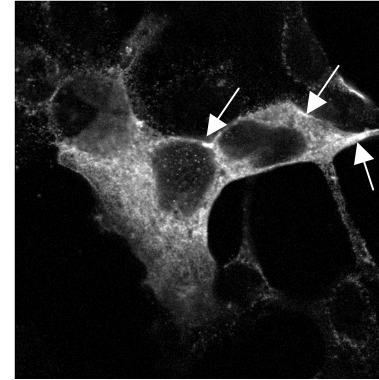


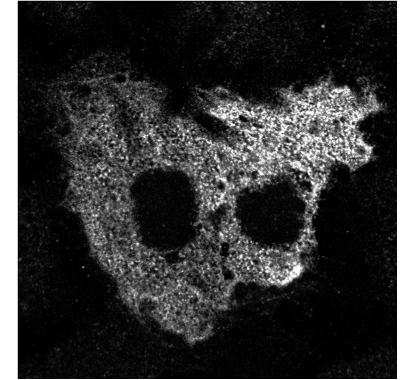
Figure 6



(b)



PDE4B5 - no tag



PDE4B5 - flag-tag

Figure 7

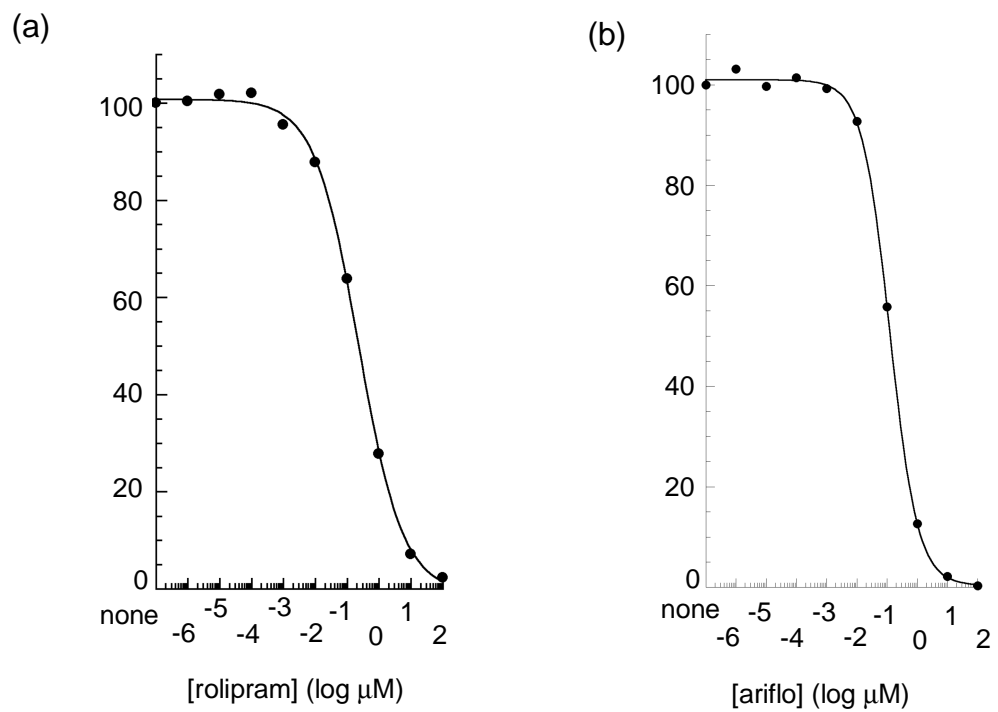


Figure 8

